Available online at www.sciencedirect.com
ScienceDirect
Journal of the European Ceramic Society 30 (2010) 465–470
www.elsevier.com/locate/jeurceramsoc

Impedance spectroscopic studies of sol–gel derived barium strontium titanate thin films

D. Czekaj *, A. Lisińska-Czekaj, T. Orkisz, J. Orkisz, G. Smalarz

University of Silesia, Department of Materials Science, 2, Sniezna St., Sosnowiec 41-200, Poland

Available online 24 July 2009

Abstract

In the present work electroceramic thin films of barium strontium titanate ($Ba_{1-x}Sr_xTiO_3$ – BST) were deposited on stainless steel substrates by sol–gel technique. Homogeneous $Ba_{0.6}Sr_{0.4}TiO_3$ thin films as well as spatially inhomogeneous BST thin films exhibiting artificial gradients in composition normal to the growth surface were deposited. Both up- and down-graded BST films were fabricated by depositing successive layers with Sr mole fraction x ranging from $x = 0.5$ to $x = 0.3$. In the present study the tool of impedance spectroscopy has been used to study the dielectric properties of BST thin films at room temperature. To analyze the impedance spectroscopy data the Nyquist (Z'' vs. Z') plots as well as the simultaneous representation of the imaginary part of impedance and electrical modulus (Z'', M'') vs. frequency were used. Experimental data were fitted using the CNLS fitting method. Agreement between experimental and simulated data was established. The data indicated that the thin film samples fabricated can be represented by an equivalent circuit with two relaxation frequencies.

Keywords: Films; Perovskites; Impedance; Spectroscopy; $Ba_{1-x}Sr_xTiO_3$

1. Introduction

The lead-free solid solution of barium strontium titanate ($Ba_{1-x}Sr_xTiO_3$ – BST) is a promising candidate for microelectronic devices that, in a thin film form, can be integrated to semiconductor technology. BST is a typical ferroelectric material exhibiting the perovskite-type structure, high dielectric constant, reasonably low dielectric loss, high dielectric breakdown strength and composition dependent Curie temperature, which can be tuned by adjusting the barium-to-strontium ratio. Another interesting feature of BST is the non-linear behavior of dielectric properties with respect to applied dc voltage. Therefore, BST thin films are suitable for tunable microwave devices operating at room temperature.[1]

The motivation of the present research was to investigate dielectric properties of homogeneous $Ba_{0.6}Sr_{0.4}TiO_3$ thin films as well as spatially inhomogeneous $Ba_{1-x}Sr_xTiO_3$ thin films exhibiting artificial gradients in composition (Sr mole fraction x ranging from $x = 0.5$ to $x = 0.3$) normal to the growth surface using impedance spectroscopy. This heterogeneous system may help to improve the dielectric properties. In this work the BST thin films of different chemical composition were grown by spin-coating deposition of metaloorganic solution.

2. Experimental procedure

Thin films of barium strontium titanate $Ba_{0.6}Sr_{0.4}TiO_3$ (BST6040) as well as compositionally graded $Ba_{1-x}Sr_xTiO_3$ (BST) thin films were fabricated by spin-coating sol–gel method and grown on polished stainless steel substrates. In this experiment, barium acetate ($Ba(CH_3COO)_2$, 99%), strontium acetate ($Sr(CH_3COO)_2$, 99%), and tetra-butyl titanate ($Ti(OC_4H_9)_4$, 97%) were used as starting materials. Glacial acetic acid (CH_3COOH) was used as a catalyst, whereas *n*-butanol ($CH_3(CH_2)_3OH$) was used as a solvent. All above reagents were of analytic purity. Details of the sol–gel process and the deposition procedure have been reported by us elsewhere [e.g.,Ref. 2].

To form a homogeneous film only a $Ba_{0.6}Sr_{0.4}TiO_3$, precursor was used. However, to form graded films with a compositional step-variation normal to the substrate the precursor solutions utilized were as follows: $Ba_{0.5}Sr_{0.5}TiO_3$, $Ba_{0.6}Sr_{0.4}TiO_3$, and $Ba_{0.7}Sr_{0.3}TiO_3$. The graded structure was formed by depositing successive layers with Sr mole fraction x ranging from $x = 0.5$ to $x = 0.3$. Final crystallization of as-deposited BST thin

* Corresponding author. Tel.: +48 323689345; fax: +48 323689563.
E-mail address: czekaj@us.edu.pl (D. Czekaj).

0955-2219/$ – see front matter © 2009 Elsevier Ltd. All rights reserved.
doi:10.1016/j.jeurceramsoc.2009.06.036

Table 1
Estimated values of resistance (R_i), capacitance (C_i), relaxation frequency ($\nu_{max,i}$) and depression angle (β_i) calculated from equivalent electric circuit parameters and equations Eqs. (7)–(9). The validity of the fitting procedure was estimated by χ^2 and WSS.

	BST567	BST765	BST6040
R_1 [Ω]	64616	2.18×10^6	3.69×10^6
C_1 [F]	1.39×10^{-8}	1.17×10^{-11}	3.62×10^{-12}
ν_{1max} [Hz]	177	6176	11888
β_1 [°]	5.70	1.79	5.59
R_2 [Ω]	130510	3.44×10^7	3.53×10^6
C_2 [F]	4.27×10^{-8}	2.86×10^{-12}	1.35×10^{-11}
ν_{2max} [Hz]	28	1613	3316
β_2 [°]	6.98	4.08	10.39
R_S [Ω]	1.99	–	–
L [H]	1.63×10^{-6}	–	–
WSS	3.75×10^{-2}	1.54×10^{-2}	7.58×10^{-2}
χ^2	1.48×10^{-4}	7.80×10^{-5}	3.86×10^{-4}

films was carried by conventional furnace annealing. For convenience, the graded films starting with $Ba_{0.7}Sr_{0.3}TiO_3$ layer at the film–substrate interface and with a $Ba_{0.5}Sr_{0.5}TiO_3$ layer at the top surface are called "down-graded" (or BST765) films, whereas the films with the opposite compositional gradient are called "up-graded" (or BST567) films.

For electric measurements the samples were covered with silver electrodes by sputtering technique through a shadow mask so as to define capacitors for electrical testing.

A Solartron 1296 Dielectric Interface and 1260 Frequency Response Analyzer were used to carry out the measurements in a frequency range 10 Hz–10 MHz at room temperature. The amplitude of the ac perturbation signal was 10 mV.

Data were fitted to the corresponding equivalent circuits with the program ZView (Scribner Associates, Inc.). The validity of the fitting procedure was estimated according to the following methods: χ-squared and the weighted sum of squares, referred to as χ^2 and WSS, respectively[3,4] (Table 1). In the present study we chose a "modulus data weighting".[4]

3. Results and discussion

BST thin films were grown on stainless steel substrates by spin-coating of the precursor solution with subsequent thermal processing. Formation of the desired perovskite-type phase was confirmed by the analysis of X-ray diffraction patterns for each sample. Observations of the thin film microstructure and results of analysis of the chemical composition show that good quality thin films were obtained by the sol–gel method.[2] It is worth noting that the compositional step-variation formed during the gradation process was not destroyed during the final thermal processing.

Impedance spectroscopy (IS) is a powerful method of characterizing many of the electrical properties of materials and their interfaces with electronically conducting electrodes.[5] A great strength of impedance spectroscopy is that, with appropriate data analysis, it is often possible to characterize the different electrically active regions in a material by demonstrating their existence and by measuring their individual electric properties.[6]

The frequency dependent properties of a material are normally described in terms of any of the formalism expressed as[5]

$$\text{Complex impedance}: \quad Z^* = Z' - jZ'' = R_S - \frac{j}{\omega C_S} \tag{1}$$

Complex admittance :

$$Y^* = Y' + jY'' = \frac{1}{R_P} + j\omega C_P = G(\omega) + jB(\omega) \tag{2}$$

$$\text{Complex permittivity}: \quad \varepsilon^* = \varepsilon' - j\varepsilon'' \tag{3}$$

$$\text{Complex modulus}: \quad M^* = (\varepsilon^*)^{-1} = M' + jM'' = j\omega C_0 Z^* \tag{4}$$

$$\text{and dielectric loss}: \quad \tan\delta = \frac{-Z'}{Z''} = \frac{Y'}{Y''} = \frac{\varepsilon''}{\varepsilon'} = \frac{M''}{M'} \tag{5}$$

where subscripts p and s refer to equivalent parallel and series circuit components, $\omega = 2\pi f$, angular frequency, C_0 is capacitance of the cell in vacuum (Z', Y', ε', M') and (Z'', Y'', ε'', M'') are the real and imaginary components of impedance, admittance, permittivity, and modulus, respectively, G: conductance, B: susceptance, and $\tan\delta$: dielectric loss.

The above expressions are interrelated with each other and offer a wide scope for graphical representation. Each representation can be used to highlight a particular aspect of the response of a sample.

The idealized plot (Z'' vs. Z'), which describes a polycrystalline oxide material, often includes three components with their corresponding relaxation frequencies. At higher frequencies, the component normally corresponds to the bulk properties (ν_b), at intermediate frequency the element corresponds to the grain boundaries (ν_{gb}), and at low frequency, we usually have the electrode processes (ν_{el}) or processes occurring at the material/electrode interface. Typically, ν_b is one or two orders of magnitude higher than ν_{gb} and ν_{el} is much smaller than ν_{gb} ($\nu_{el} \ll \nu_{gb} \ll \nu_b$).[7,8] In real oxide systems this behavior may be rather complicated due to the different factors which influence the bulk and the grain boundary properties—chemical composition, impurities, ageing, and technological conditions.

When overlapping between processes increases, one may need alternative representations such as those based on the modulus, admittance, and permittivity[6], or based on combined spectroscopic plots of the imaginary components of impedance, Z'' and electric modulus M'',[9,10] or representation of $\log(\tan(\delta))$ vs. $\log(\nu)$ to reveal the bulk, grain boundary and electrode components of impedance spectra,[11] using the derivative of the tangent of the phase angle to discriminate different electrode processes,[8,12] or inspection of alternative Z' vs. Z''/ν representations which is mainly useful to characterize the grain boundary to electrode transition and to assess the electrode relaxation frequency.[13] The derivative $dZ'/d(Z''/\nu)$ may be an alternative representation for materials with a significant distribution of relaxation frequencies in the grain boundary range, and to reveal the onset of the bulk and/or electrode terms when the Nyquist plot is largely dominated by very resistive grain boundaries.[13]

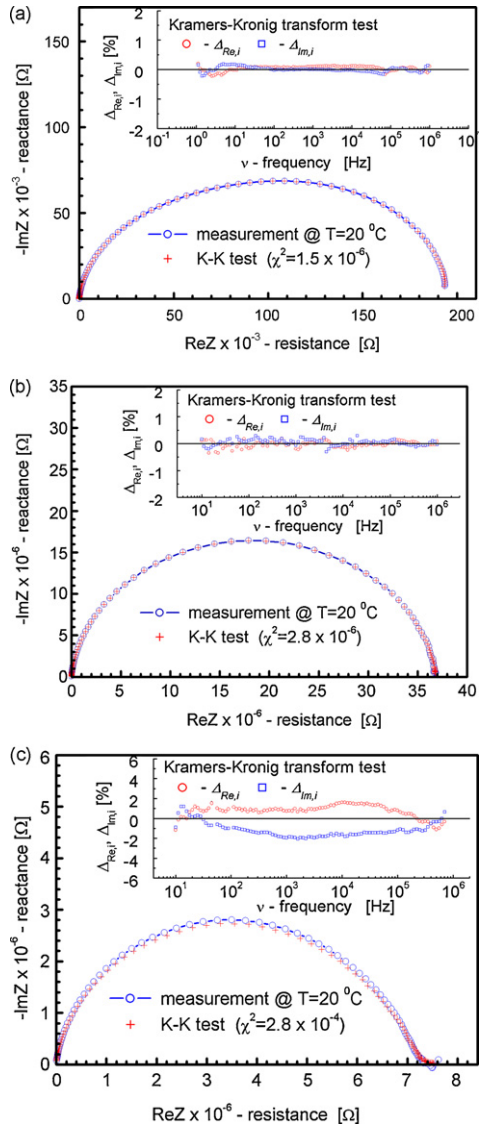

Fig. 1. Impedance diagram for BST567 (A) BST765 (B) and BST6040 (C) thin film (open circles, measured data; crosses, Kramers–Kronig transform test results). The inset shows results of K–K test in the form of the relative differences plot.

It is worth remarking that it would be ideal to use only one type of representation to obtain both qualitatively the number of processes and the parameters that characterize them or at least the relationships between these parameters that could be used with other non-linear fitting methods to refine the proposed circuit.

In order to extract from impedance measurements as much information as possible the experimental spectra, given in Fig. 1A–C were subjected to a preliminary inspection. Visual analysis of the plots of individual IS data have shown that the experimental points form smooth curve(s) (Fig. 1, open circles). The most important aspect is whether the given spectra really represents the impedance (proportionality coefficient between the related electric potential and current). In the present study the analysis by the Kramers–Kronig (K–K) relations has been used to validate the data with the use of the computer program by Boukamp.[14–16]

The inset of Fig. 1 displays results of K–K test in the form of the relative differences plot. The resulting "pseudo Chi-squared" value is shown in the figure. A random distribution around the frequency axis indicates that the data is K–K compliant[17] (Fig. 1A and B). A clear trace, as indicated in the inset of Fig. 1C, shows that there is non-K–K behavior, however, it is quite small as the residuals are less than 2%. In Fig. 1 one can see displayed the combination of the measured data (open circles) and its K–K transformation (crosses).

From the visual inspection of IS data, given in Fig. 1, one can see that the complex plot is in a form of one depressed semicircle, starting from the origin, making an intercept on the real axis with a large radius (and a small tail at low frequencies for BST6040 thin film – Fig. 1C). Therefore, to resolve the overlapped processes, the combined usage of impedance and modulus spectroscopic plots was used, as suggested in the literature.[9] The advantage of this technique being that the M'' and Z'' (the imaginary parts of modulus and impedance, respectively) peaks for a particular RC combination should be coincident on the frequency scale (ideal Debye case). Hence the power of combined usage of impedance and modulus spectroscopy is that the Z'' plot highlights phenomena with the largest resistance whereas M'' picks out those with smallest capacitances.

Fig. 2 depicts the simultaneous variation of Z'' and M'' with frequency. A preliminary glance at these plots, shown in Fig. 2A–C, shows that there are departures from the ideal Debye behavior. A closer observation of these plots reveals the following: (i) for BST567 Z'' plot peaks at $\nu = 40$ Hz, and M'' plot peaks at $\nu = 200$ Hz (Fig. 2A); (ii) for BST765 Z'' plot peaks at $\nu = 1778$ Hz, whereas M'' plot peaks at $\nu = 2238$ Hz (Fig. 2B), and (iii) in the case of BST6040 thin film Z'' plot peaks at $\nu = 7943$ Hz, and M'' plot peaks at $\nu = 14125$ Hz (Fig. 2C). It is worth noting that BST567 and BST765 graded thin films have been prepared at the same processing conditions and they differ in the direction of the chemical composition gradient.

The elements of an equivalent circuit model represent the various (macroscopic) processes involved in the transport of mass and charge. Equivalent circuits used for impedance spectroscopy data simulation in the present study were composed of resistors, R, inductors, L, and constant phase elements, CPE (symbol: Q) (Fig. 3A – for simulation of IS data for BST567 thin film; Fig. 3B – BST765 and BST6040 thin films). In solid materials, a distribution of relaxation times is usually observed and the capacitance is replaced by a CPE, which represents more accurately the behavior of the grain interior, grain boundary and electrode processes.[18] A CPE is characterized by two parameters. The admittance $Y(\omega)$, of CPE can be defined as follows:

$$Y^*(\omega) = T(j\omega)^P \tag{6}$$

where coefficient T and the exponent P $(-1 < T < 1)$ are two specific parameters of the CPE. The CPE causes depression of the ideal semicircle, observed on the complex plane plots by an angle:

$$\beta = (1 - P)\frac{\pi}{2} \tag{7}$$

where β is the depression angle.

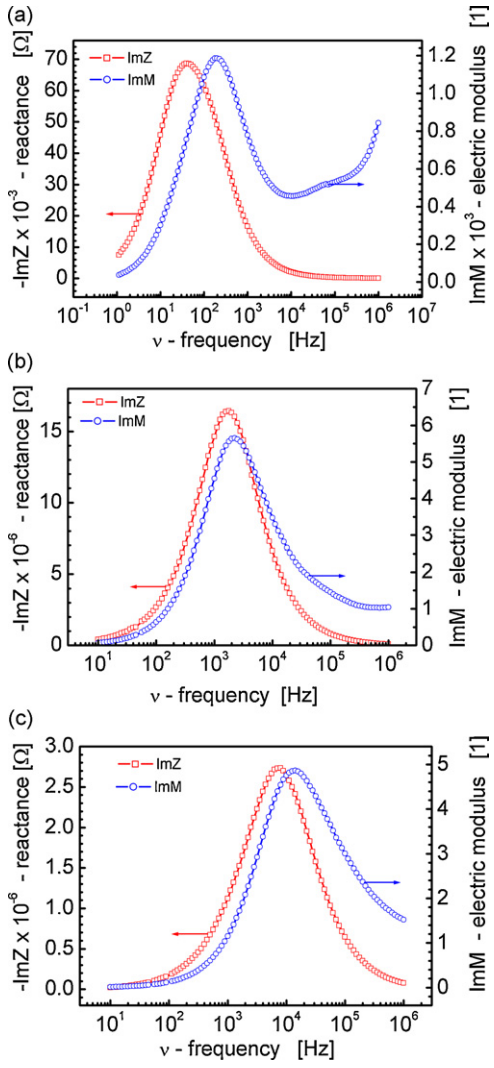

Fig. 2. Dependence of Z'' and M'' on frequency for BST567 (A) BST765 (B) and BST6040 (C) thin film.

Results of the simulation performed according to the complex non-linear least squares method (CNLS),[14] are given in Fig. 4A–C for BST567, BST765 and BST6040, respectively. One can see agreement between the measured and simulated data.

After performing the impedance spectroscopy data simulation, the calculated values of the equivalent electric circuit parameters were then related to the characteristic parameters of the (macroscopic) processes according to the following relations[3,19]:

$$\nu_{max} = \frac{1}{2\pi(RT)^{1/P}} \tag{8}$$

$$C = \frac{1}{2\pi R \nu_{max}} \tag{9}$$

where ν_{max} is a relaxation frequency, R and C are resistance and capacitance of the bulk or grain boundary or electrode processes contribution to the impedance data.

Results of the data simulation in a form of estimated parameters of the relaxation processes are given in Table 1.

Although the technological conditions of the thin films fabrication were kept identical the measured impedance spectra show estimated relaxation frequencies in different frequency ranges: low frequency range for up-graded BST567 thin film (resistance $\sim 10^4$ to $10^5\ \Omega$, and capacitance $\sim 10^{-8}$ F) and medium frequency range for down-graded BST765 thin film (resistance $\sim 10^6$ to $10^7\ \Omega$, and capacitance $\sim 10^{-11}$ to 10^{-12} F) and BST6040 thin film. Taking into consideration the magnitude of the capacitances[8,10] we suppose that the main contribution to the impedance spectra of up-graded thin film is done by grain boundaries and/or electrode processes whereas for down-graded and BST6040 thin film—the main contribution is done by the bulk processes.

The difference in the relaxation processes which dominate the dielectric response of the up-graded and down-graded BST thin films may be understood in terms of the effect of both grain size and stress induced during grain growth,

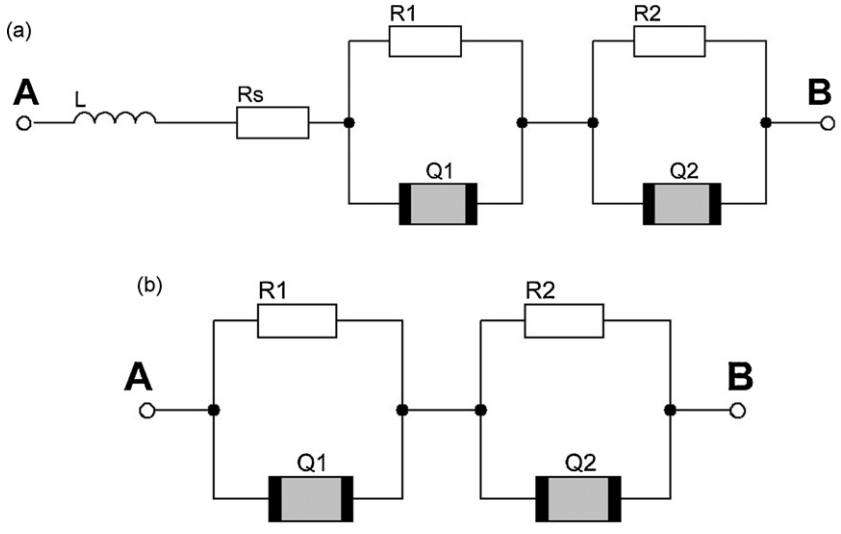

Fig. 3. Schematic representation of the equivalent circuit used in the dispersion analysis for BST567 thin film (A) and for BST765 and BST6040 thin films (B).

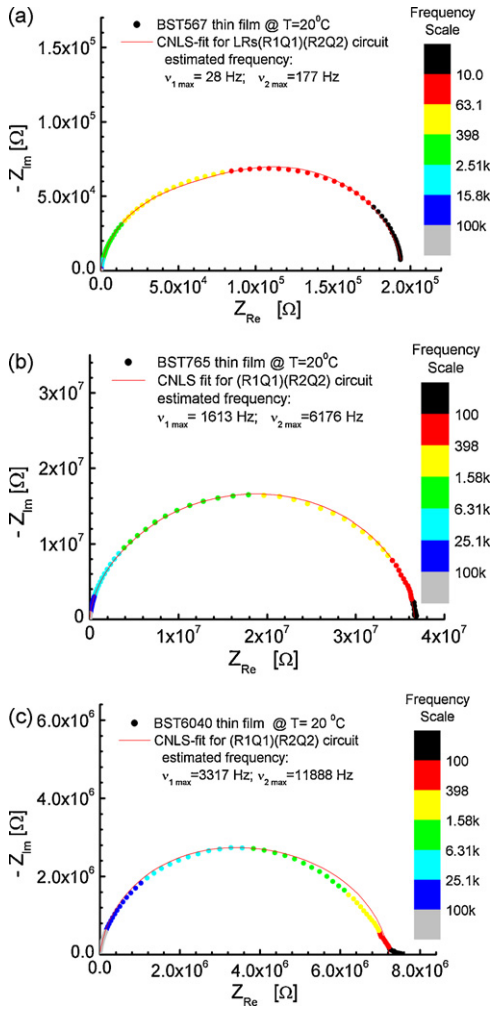

Fig. 4. Plot of Z'' vs. Z' for BST567 (A) BST765 (B) and BST6040 (C) thin film. Combination of the measured data (circles) and its CNLS-fit (line) is given.

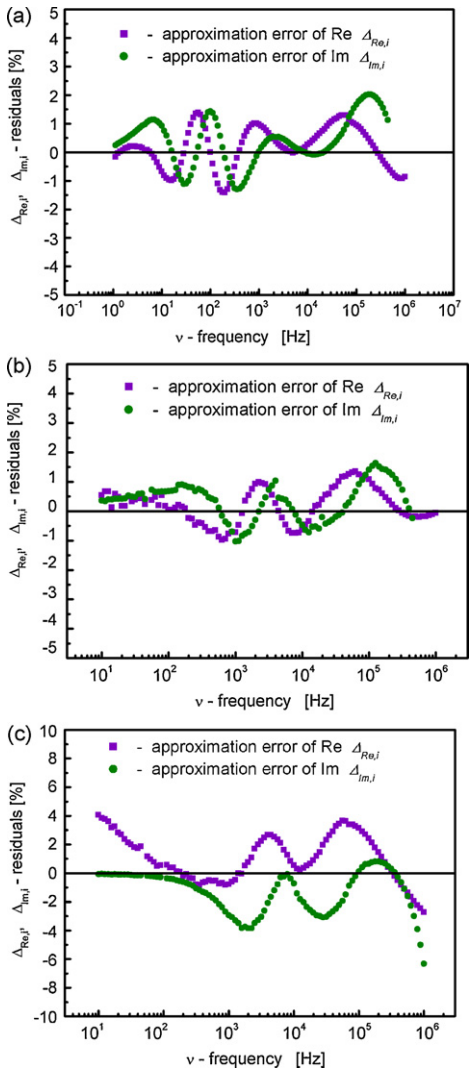

Fig. 5. FQ-plot for the final parameter set obtained with the dispersion analysis program for BST567 (A), BST765 (B) and BST6040 (C) thin film.

which significantly depends upon the substrate material used. Especially, the thin films fabricated by the sol–gel technique are known to exhibit the characteristic of substrate-sensitive crystallization.[20,21] In our study the bottom layer of up-graded films (i.e., the $Ba_{0.5}Sr_{0.5}TiO_3$ layer) had served not only as part of grade film but also as a seeding layer for enhancing fine-grained crystallization of the subsequent film layers. Therefore, it is reasonable to suppose that the different crystallization kinetics process is the main cause that the dielectric response of the down-graded BST765 films at room temperature is dominated by bulk processes whereas for up-graded BST567 films the main role is played by the grain boundary and/or electrode processes.

The quality of the parameter fit of an equivalent circuit to a set of impedance data can be best seen in a fit quality plot (FQ-plot)[14] in which the relative deviations of the real, Δ_{Re}, and imaginary part, Δ_{Im}, of the impedance are plotted against frequency (ν) on a log scale (Fig. 5A–C). For a good fit these deviations should be distributed randomly around the frequency axis. In our experiment a clear sinusoidal-type trace is seen in Fig. 5, however, the residuals for both up- and down-graded BST thin films are less than 2%, whereas for BST6040—the residuals are less than 5%. In this connection it is worth noting that the estimations of the validity of the simulations, namely χ-squared (χ^2) and the weighted sum of squares (WSS), given in Table 1 show rather good quality of the simulations performed in the course of this study. Their values ($\chi^2 \sim 10^{-4}$ to 10^{-5} and WSS $\sim 10^{-2}$) are in good agreement with other published results.[3]

4. Conclusions

Thin films of $Ba_{0.6}Sr_{0.4}TiO_3$ as well as both down- and up-graded BST thin films (Sr content x increasing toward the top electrode and toward the bottom electrode, respectively) were successfully grown by sol–gel method on stainless steel substrates. The impedance spectroscopy data validation, both visual and performed by Kramers–Kronig test, shows that the measured data reflects the sample impedance.

All the samples under investigation have shown two relaxation processes at room temperature. The corresponding equivalent circuits consist of two parallel R-CPE elements connected in series. In case of BST567 thin film the inductance L

was included in the equivalent circuit to take into consideration high frequency contribution, due to the instrumentation.

Results of the simulation show good agreement between the measured and simulated data. Although the FQ-plots show a clear sinusoidal-type trace the residuals are less than 5% and parameters of validation namely, χ-squared and the weighted sum of squares are reasonably low.

On the basis of the estimated capacitances and the relaxation frequencies we suppose that the main contribution to the impedance spectra of up-graded BST thin film is done by grain boundaries and/or electrode processes whereas for down-graded and BST6040 thin film—the main contribution is done by the bulk processes. However, the authors realize that in case of ferroelectric materials study of thermal dependencies of the calculated capacitances will be helpful for distinguishing ferroelectric components from the non-ferroelectric ones and such a study is planned for compositionally graded barium strontium titanate thin films.

Acknowledgements

The authors wish to acknowledge Polish Ministry of Education and Science for financially supporting the present research from the funds for science in 2006–2009 as a research project N507 098 31/2319. The authors would like to thank Professor Marta Radecka, Department of Inorganic Chemistry, Faculty of Materials Science and Ceramics, AGH University of Technology, Krakow for extending experimental facilities.

References

1. Vendik, O. G., Ter-Martirosyan, L. T., Dedyk, A. I., Karmanenko, S. F. and Chakalov, A., High-T_c superconductivity: new applications of ferroelectrics at microwave frequencies. *Ferroelectrics*, 1993, **144**, 33–43.
2. Orkisz, T., Czuber, J., Lisińska-Czekaj, A., Adamczyk, M. and Czekaj, D., Zastosowanie technologii zolowo-żelowej do otrzymywania cienkich warstw $Ba_{1-x}Sr_xTiO_3$. *Polski Biuletyn Ceramiczny, Ceramika/Ceramics*, 2008, **101**, 285–293.
3. Guillodo, M., Fouletier, J., Dessemond, L. and Del Gallo, P., Electrical properties of dense Me-doped bismuth vanadate (Me = Cu, Co) pO_2-dependent conductivity determined by impedance spectroscopy. *J. Eur. Ceram. Soc.*, 2001, **21**, 2331–2344.
4. Zoltowski, P., Non-traditional approach to measurement models for analysis of impedance spectra. *Solid State Ionics*, 2005, **176**, 1979–1986.
5. Barsoukov, E. and Ross Macdonald, J., ed., *Impedance Spectroscopy, Theory, Experiment, and Applications*. 2nd ed. John Wiley & Sons, Inc., Publication, 2005.
6. West, A. R., Sinclair, D. C. and Hirose, N., Characterization of electrical materials, especially ferroelectrics, by impedance spectroscopy. *J. Electroceram.*, 1997, **1**(1), 65–71.
7. Abrantes, J. C. C., Labrincha, J. A. and Frade, J. R., Representation of impedance spectra of ceramics. Part I. Simulated study cases. *Mater. Res. Bull.*, 2000, **35**, 955–964.
8. Ruiz-Morales, J. C., Marrero-Lopez, D., Irvine, J. T. S. and Nunez, P., A new alternative representation of impedance data using derivative of the tangent of the phase angle. Application to YSZ system composites. *Mater. Res. Bull.*, 2004, **39**, 1299–1318.
9. Sinclair, D. C. and West, A. R., Impedance and modulus spectroscopy of semiconducting $BaTiO_3$ showing positive temperature coefficient of resistance. *J. Appl. Phys.*, 1989, **66**, 3850–3856.
10. Irvine, J. T. S., Sinclair, D. C. and West, A. R., Electroceramics: characterization by impedance spectroscopy. *Adv. Mater.*, 1990, **2**, 132–138.
11. Abrantes, J. C. C., Labrincha, J. A. and Frade, J. R., Representation of impedance spectra of ceramics. Part II. Spectra of polycrystalline $SrTiO_3$. *Mater. Res. Bull.*, 2000, **35**, 965–976.
12. Ruiz-Morales, J. C., Marrero-Lopez, D., Canales-Vasquez, J., Nunez, P. and Irvine, J. T. S., Application of an alternative representation to identify models to fit impedance spectra. *Solid State Ionics*, 2005, **176**, 2011–2022.
13. Abrantes, J. C. C., Labrincha, J. A. and Frade, J. R., An alternative representation of impedance spectra of ceramics. *Mater. Res. Bull.*, 2000, **35**, 727–740.
14. Boukamp, B., A nonlinear least squares fit procedure for analysis of immittance data of electrochemical systems. *Solid State Ionics*, 1986, **20**, 31–44.
15. Boukamp, B. A., Practical application of the Kramers–Kronig transformation on impedance measurement in solid state electrochemistry. *Solid State Ionics*, 1993, **62**, 131–141.
16. Boukamp, B. A., Electrochemical impedance spectroscopy in solid state ionics: recent advances. *Solid State Ionics*, 2004, **169**, 65–73.
17. Boukamp, B. A., A linear Kronig–Kramers transform test for immitance data validation. *J. Electrochem. Soc.*, 1995, **142**, 1885–1894.
18. Lasia, A., Electrochemical impedance spectroscopy and it's applications. In *Modern Aspects of Electrochemistry*, *vol. 32*, ed. B. E. Conway, J. O'. M. Bockris and R. E. White. Kluver Academic/Plenum Publishers, New York, 1999, pp. 143–248.
19. Brug, G. J., Van den Eeden, A. L. G., Sluyters-Rehbach, M. and Sluyters, J. H., The analysis of electrode impedances complicated by the presence of a constant phase element. *J. Electroanal. Chem.*, 1984, **176**, 275–295.
20. Jiwei, Z., Xi, Y., Liangying, Z., Bo, S. and Chen, H., Dielectric properties of the compositionally graded (Ba,Sr)TiO_3 thin film. *Ferroelectrics*, 2005, **329**, 43–48.
21. Bao, D., Mizutani, N., Yao, X. and Zhang, L., Dielectric and ferroelectric properties of compositionally graded (Pb,La)TiO_3 thin films on Pt/Ti/SiO_2/Si substrates. *Appl. Phys. Lett.*, 2000, **77**(8), 1203–1205.